PHYSICAL REVIEW B VOLUME 35, NUMBER 10 1 APRIL 1987

# Properties of model-valence-fluctuation heavy-electron systems in applied and molecular fields

D. L. Cox*
*Physics Department, B019, University of California, San Diego, La Jolla, California 92093*
(Received 20 June 1986)

Self-consistent large-orbital-degeneracy perturbation theory for the one-site Anderson model is used to compute the occupancy and magnetization as a function of field and temperature for both spin $\frac{1}{2}$ and spin $\frac{5}{2}$. The magnetization curves are in good agreement with exact Bethe-ansatz and high-field perturbation-theory results, although some systematic discrepancies are apparent between the two different approaches. The most novel result for the magnetization is that the "superlinear" behavior known for high-degeneracy impurities (and observed in YbCuAl) vanishes at precisely the temperature where the zero-field magnetic susceptibility peaks. The one-impurity results are extended to the lattice via perturbation theory in the intersite interactions, after which simple molecular field theory (excluding the possibilities of charge-density wave and superconducting phases) is applied to obtain magnetic-ordering phase boundaries for the spin-$\frac{1}{2}$ and spin-$\frac{5}{2}$ models which are in gross qualitative agreement with previous lattice calculations, including the so-called "Kondo necklace" and "resonant level" models. In particular, the criterion that the intersite coupling exceed the characteristic Kondo-effect energy scale is recovered. It is shown that the superlinear behavior obtained for high-degeneracy leads, within molecular field theory, to novel tricritical behavior without the inclusion of anisotropy terms. It is suggested that $EuRh_3B_2$ and YbCuAl are likely candidates for observing this behavior. Detailed appendices indicate the approximations necessary to obtain the molecular field theory and thereby its limitations to finite temperatures away from the coherent regime of the Anderson lattice.

## I. INTRODUCTION

This paper is devoted to a study of the response of a model valence-fluctuating heavy-electron site to applied magnetic fields or to internal molecular fields. Calculations are performed with the degenerate Anderson model[1] via the recently developed self-consistent large-orbital-degeneracy perturbation theory.[2–9] Particular attention is paid to the high-degeneracy limit at finite field and temperature, which only recently has been treated by the Bethe-ansatz approach.[10]

The large-orbital-degeneracy perturbation theory has allowed reliable calculations of static and dynamic properties of the degenerate Anderson model.[11–13] Previously, the numerical renormalization group had yielded essentially exact results for the magnetic susceptibility and specific heat of the one-impurity spin-$\frac{1}{2}$ Kondo model[14] and the magnetic susceptibility of the spin-$\frac{1}{2}$ Anderson model.[15] The Bethe ansatz has yielded exact calculations of all static properties of the one-impurity Kondo[16,17] and Coqblin-Schrieffer[18,19] models as well as both the nondegenerate[20] and degenerate[21] Anderson models. Comparison of the magnetic susceptibility and specific heat calculated within the degenerate Anderson model via the self-consistent perturbation theory shows excellent agreement with both renormalization-group and Bethe-ansatz results,[12] even when the susceptibility and magnetization curves for degeneracy 2 are compared (this paper). This latter surprising applicability of large-$N_{\rm grd}$ theory to spin $\frac{1}{2}$ has been noted previously.[22,23]

Another development which has arisen both empirically and been suggested theoretically via large orbital degeneracy arguments is that the one-site model has considerable relevance for the lattice. Namely, alloying studies [of which $Ce_xLa_{1-x}Al_2$ (Ref. 24) and $Ce_xLa_{1-x}Pb_3$ (Ref. 25) provide the most compelling examples] show that experimental properties such as the specific heat, magnetic susceptibility and high-temperature resistivity scale almost perfectly with the concentration of the valence-fluctuating, heavy-electron sites all the way from the dilute to concentrated limits. Qualitative theoretical arguments have been put forth which point out that large degeneracy significantly enhances the characteristic Kondo effect energy relative to the (perturbative) estimates of the intersite couplings.[26–28] The formation of $4f$ bands does not appear to mitigate these conclusions for static properties, at least within the simplest variational calculations, although clearly transport properties must (in view of Bloch's theorem) begin to be modified at some low-temperature scale.[29,30] In addition, there is some experimental evidence for the breakdown of one-site behavior at very low-temperature scales ($\sim 1$ K or less in the heavy-electron systems) in even static properties which can plausibly be attributed to coherent lattice effects.[31]

Valence-fluctuation and heavy-electron materials are quite remarkable for the presence of high-mass fermi-liquid behavior reflected in giant linear specific-heat coefficients and zero temperature Pauli susceptibilities,

 

ranging from 10 to 1000 times normal metallic values.[25,32,33] As is now well known, some of these materials ($CeCu_2Si_2$, $UPt_3$, and $UBe_{13}$) exhibit unusual superconductivity with giant critical field slopes and specific heat jumps, all consistent with the above picture of a heavy Fermi liquid.

However, while this Fermi-liquid state is heavy, it is usually only mildly enhanced in the sense of magnetic interactions. Indeed, what is perhaps most surprising is the absence of magnetic order in many of these materials despite the presence of highly localized $f$ electrons with well-defined free-ion moments. Conventional wisdom suggests that the strong spin and charge fluctuations induced by hybridization with conduction electrons tend to strongly favor a paramagnetic ground state.

Experimentally, those compounds which appear to possess valence-fluctuation and/or heavy-electron anomalies for temperatures above some magnetic ordering fall roughly into the following two classes. (i) Those which appear to be grossly describable in terms of localized moments interacting via some exchange interaction [presumably the Ruderman-Kittel-Kasuya-Yosida (RKKY) conduction-electron mediated exchange]. Although these systems may still possess anomalies which contrast with normal magnetic rare-earth metals, a list of such materials might include $EuRh_3B_2$,[34,35] $CeAl_2$,[36,37] $CeB_6$ (below the quadrupolar ordering temperature),[38] and $CePb_3$.[39] (ii) Those which show behaviors reminiscent of itinerant magnets, namely, reduced moment ordering, mean-field-like specific-heat jumps, and anomalous effective Curie moments near $T_c$ (for ferromagnetic ordering). $CeIn_3$,[40] $CeRh_3B_2$,[41] and $U_2Zn_{17}$, (Refs. 42 and 43) might fall within this category. I note that while itinerant magnetism might look like an appropriate interpretation, neutron scattering measurements show apparently well-defined ordered structures residing on the rare-earth or actinide sublattices in $U_2Zn_{17}$ (Ref. 43) and $CeIn_3$ (Ref. 44). Presumably, a clear discrimination between local and itinerant behavior would require careful examination of the magnetic form factor at long wavelengths.[45]

This paper reports on an application of the molecular field theory of magnetic ordering to the Anderson lattice model for valence-fluctuation, heavy-electron materials in the extreme local moment limit. The purpose of this work is to simply study the competition between the Kondo effect which favors the paramagnetic state and intersite exchange coupling which favors magnetic order. The possibility of competing charge-density-wave or superconducting states is not considered here. Within the simple calculational framework used here, all effects are controlled by the ratio of the molecular field exchange strength $\lambda$ to the characteristic Kondo effect energy $T_L$. For (i) $\lambda/T_L \gg 1$, normal local moment ordering is approached; (ii) for $\lambda/T_L \ll 1$, paramagnetic order ensues; (iii) for $\lambda/T_L \sim 1$, magnetic ordering can occur, but is characterized by reduced spontaneous (or staggered) magnetization, low transition temperature, and for ferromagnetic order, enhanced effective Curie moments. Such behavior is reminiscent of itinerant magnetism.

Previous studies of the Kondo or Anderson lattice models reached similar conclusions about the interplay of the Kondo effect and intersite interactions. Doniach's variational treatment of the related "Kondo necklace" model showed a ground-state boundary between on-site singlet behavior and antiferromagnetic order.[46] While subsequent calculations have apparently mitigated the conclusions of this early work,[47] the qualitative picture which emerged is still used for conceptual descriptions of magnetically ordered valence-fluctuation, heavy-electron systems. Calculations for the two impurity Kondo and Anderson models[48,49] showed that if the intersite RKKY coupling was less than the Kondo temperature, on-site singlet formation would occur before any formation of extended local moments. Molecular-field calculations for the noninteracting resonant level model often used to phenomenologically parameterize the experimental data yielded the same qualitative picture.[36,37]

An additional feature of interest arises in regime (iii) above. Namely, a novel kind of tricritical point appears for orbital degeneracy higher than 3 which requires no anisotropy terms in the free energy. Such behavior is directly traceable to low-temperature "superlinear" behavior in the magnetization, the relevance of which has been pointed out before in the context of the Anderson lattice model and the formation of real and/or pseudogaps in the electronic density of states.[50] Here the behavior is seen as an intrinsic feature of the one-site model traceable to the "inelastic" nature of the "Kondo resonance" for high degeneracy. Despite the simplistic nature of these calculations, there are encouraging reasons to believe that such a novel tricritical effect might be observable in $EuRh_3B_2$ and YbCuAl; these will be discussed in detail in the text.

It should be noted that the perturbation theory in the intersite interactions does not include coherent modifications (discussed in Refs. 28–30) necessary for a treatment of magnetic ordering close to the ground state (which could include the possibility of spin-density-wave formation). This point is elucidated in Appendix A. Hence, conclusions reached here are restricted to ordering temperatures above the ground state. No clear criterion is derived here for distinguishing coherent, itinerant magnetism amongst heavy electrons from ordering closer conceptually to that of a lattice of local moments.

The outline of the paper is as follows. Section II contains a brief review of the degenerate Anderson model and the self-consistent perturbation theory approach. Section III presents the results for the temperature- and field-dependent occupancies and magnetization for both the spin-$\frac{1}{2}$ and spin-$\frac{5}{2}$ Anderson models. Section IV contains a calculation of phase diagrams and other properties related to magnetic ordering via the application of simple molecular field theory to the one-site free energy. Section V contains a summary and conclusions. Appendix A contains a derivation of the molecular field theory of Sec. IV by use of the functional integral formalism which clearly illustrates the structure and limitations of the theory. Appendix B contains a perturbative estimate of the intersite coupling which illustrates why for the heavy-electron systems in which the competition between the Kondo effect and intersite coupling is expected to be most acute that the normal RKKY interaction between moments is expected to be most relevant.

## II. MODEL AND METHOD

### A. Degenerate Anderson model

The degenerate Anderson model Hamiltonian in the $U\rightarrow\infty$ limit may be decomposed into four terms as follows:

$$H=H_c+H_f+H_{cf}+H_z \ . \tag{2.1}$$

The first term is simply that of the (noninteracting) conduction band given by

$$H_c=\sum_{k\sigma}\epsilon_k c^{\dagger}_{k\sigma}c_{k\sigma} \ . \tag{2.2}$$

In the calculations of this paper the conduction band is taken to be half-filled with a simple Lorentzian density of states profile $N(\epsilon)=N(0)D^2/(\epsilon^2+D^2)$. The pseudoatomic $f$ electron Hamiltonian is given by

$$H_f=\sum_m \epsilon_f \mid m\rangle\langle m \mid +\epsilon_0 \mid 0\rangle\langle 0 \mid \ . \tag{2.3}$$

Here of course $m$ indexes the $N_{\rm grd}=2j+1$ degenerate $f^1$ states, and $\mid 0\rangle$ is the empty $f$ orbital. Since only the interconfigurational energy difference is relevant to the physics, I henceforth set $\epsilon_0$ equal to zero. The hybridization term $H_{cf}$ is given by

$$H_{cf}=\sum_{k,\sigma,m}\frac{V_k}{N_s^{1/2}}(c^{\dagger}_{km}\mid 0\rangle\langle m \mid +\text{H.c.}) \ . \tag{2.4}$$

Henceforth, I shall drop the $k$ dependence of the hybridization and parametrize it in terms of the width

$$\Gamma=\pi N(0)V^2 \ .$$

The conduction operator $c_{km}$ above is the appropriately symmetry-projected piece of the full Bloch-state operator—e.g., if I have a $j=\frac{5}{2}$ Ce orbital, then

$$c_{km}=\sum_{\sigma}\int\frac{d\hat{k}}{4\pi}\langle 3,m-\sigma;\tfrac{1}{2},\sigma \mid jm\rangle Y_{3m-\sigma}(\hat{k})c_{k\sigma} \ . \tag{2.5}$$

Finally, the Zeeman term $H_z$ is just given by

$$H_z=\sum_m g_j\mu_B h_z m \mid m\rangle\langle m \mid +\sum_{k\sigma}g_c\mu_B h_z n_{k\sigma} \tag{2.6}$$

in an applied field $h_z$. In subsequent calculations I shall ignore the conduction-electron polarization implied by the second term of (2.6) since it perturbatively small.[51]

### B. Method

The self-consistent perturbation theory has been reviewed elsewhere extensively (Refs. 2–8), and so I shall remind the reader of only the essential features here. While many techniques have been used to derive the central equations of the theory, the most transparent is probably the pseudoparticle approach of Barnes and Coleman.[8,52] In this approach, all projection operators in the Hamiltonian are replaced by products of pseudofermion operators $f_m$ for the $f^1$ states and pseudoboson operators for the $f^0$ state. For example, $\mid 0\rangle\langle m \mid$ becomes $b^{\dagger}f_m$. A chemical potential term $-\lambda(\sum_m f^{\dagger}_m f_m+b^{\dagger}b)$ is added and at the end of all calculations to project to the physical subspace in which the "charge" conjugate to $\lambda$ is unity (corresponding to the restriction of no double occupancy) $\lambda$ is taken to $-\infty$.

With this prescription for the Hamiltonian and subsequent calculations, all relevant terms in perturbation theory can be computed with standard Feynman-Dyson–type diagrammatics augmented by a final projection to the physical subspace. The basic building blocks of the perturbation theory are the pseudofermion and pseudoboson spectral functions $A_m(\omega,T)$ and $B(\omega,T)$ which are defined by

$$-\lim_{\lambda\rightarrow-\infty}\int d\tau e^{i(z-\lambda)\tau}\langle Tf_m(\tau)f^{\dagger}_m\rangle=\int\frac{d\omega}{\pi}\frac{A_m(\omega,T)}{z-\omega} \tag{2.7}$$

and

$$-\lim_{\lambda\rightarrow-\infty}\int d\tau e^{i(z-\lambda)\tau}\langle Tb(\tau)b^{\dagger}\rangle=\int\frac{d\omega}{\pi}\frac{B(\omega,T)}{z-\omega} \ . \tag{2.8}$$

In terms of these spectral functions, it can be shown that the total partition function factors into a product $Z_{\rm CB}Z_f$ where $Z_{\rm CB}$ is just the ordinary conduction-electron grand partition function, and $Z_f$ is given by

$$Z_f(T)=\int\frac{d\omega}{\pi}\left[\sum_m A_m(\omega,T)+B(\omega,T)\right]e^{-\beta\omega} \ . \tag{2.9}$$

Here, $\beta=1/k_BT$ as usual. Note that $Z_f$ has the physically plausible form of generalized Boltzmann statics with the $f$ configurational spectra ordinarily represented by $\delta$ functions broadened into continua by the hybridization with conduction electrons.

One may define self-energies $\sigma_m(\omega,T)$ and $\Pi(\omega,T)$ for the pseudofermion and pseudoboson spectra according to

$$\int\frac{d\omega}{\pi}\frac{A_m(\omega,T)}{z-\omega}=[z-\epsilon_f-\sigma(z,T)]^{-1}=g_m(z,T) \tag{2.10}$$

and

$$\int\frac{d\omega}{\pi}\frac{B(\omega,T)}{z-\omega}=[z-\Pi(z,T)]^{-1}=D(z,T) \ . \tag{2.11}$$

The self-consistent perturbation theory used here consists in solving the coupled integral equations

$$\sigma(\omega+i\eta,T)=\frac{\Gamma}{\pi}\int\frac{d\omega'}{\pi}B(\omega',T)K(\omega-\omega'+i\eta,T) \tag{2.12}$$

and

$$\Pi(\omega+i\eta,T)=\frac{\Gamma}{\pi}\sum_m\int\frac{d\omega'}{\pi}A_m(\omega',T)K(\omega-\omega'+i\eta,T) \ . \tag{2.13}$$

Here $\eta$ is a positive infinitesimal and the integral kernel $K(z,T)$ is given by

$$K(z,T)=\int d\epsilon \frac{N(\epsilon)}{N(0)}\frac{f(\epsilon)}{z-\epsilon}\ , \tag{2.14}$$

$f(\epsilon)$ being $(e^{\beta\epsilon}+1)^{-1}$.

The physical origin of Eqs. (2.12) and (2.13) is rather clear; they are the simplest self-consistent processes corresponding to, e.g., destruction of a pseudoboson or $f^0$ state to create a $f^1$ particle, conduction-electron hole state through hybridization. However, vertex corrections are explicitly neglected in the equations and this omission leads to some pathological behavior on low-temperature and energy scales which will be discussed momentarily.

While the pseudoparticle spectra are of some interest in their own right and do obviously contribute to the partition function, they are in no way directly observable. Only two particle correlation functions of the pseudoparticle spectra give rise to measurable properties. The ones which shall directly concern us here are the $4f$ spectral density and the magnetic susceptibility. The spectral density $\rho_m(\omega,T)$ is defined in terms of the "full $f$ Green's function" $G_m(z)$ given by

$$\begin{aligned}G_m(z)&=-\int d\tau e^{iz\tau}\langle T[\,|0\rangle\langle m\,|(\tau)]\,|m\rangle\langle 0\,|\,\rangle\\&=\int\frac{d\omega}{\pi}\frac{\rho_m(\omega,T)}{z-\omega}\ .\end{aligned} \tag{2.15}$$

The spectral density is of course the particle addition spectrum for positive frequency, and the particle removal spectrum for negative frequency. At the level of approximation of Eqs. (2.12) and (2.13), the spectral function is given by the formula

$$\begin{aligned}\rho_m(\omega,T)=&\frac{1}{Z_{4f}(T)}\\&\times\int\frac{d\omega'}{\pi}e^{-\beta\omega'}[A_m(\omega'+\omega,T)B(\omega',T)\\&\qquad+A_m(\omega',T)B(\omega'-\omega,T)]\ .\end{aligned} \tag{2.16}$$

From Eq. (2.16) two useful sum rules immediately follow. First, the $4f$ occupancy $n_f(T)$ is given by

$$\begin{aligned}n_f(T)&=\sum_m\int\frac{d\omega}{\pi}f(\omega)\rho_m(\omega,T)\\&=\frac{1}{Z_{4f}(T)}\sum_m\int\frac{d\omega}{\pi}e^{-\beta\omega}A_m(\omega,T)\ .\end{aligned} \tag{2.17}$$

Secondly, the $4f$ polarization (the magnetization reduced by the high-field saturation value) $\mathbf{M}_0(T,H)$ is given by

$$\begin{aligned}M_0(T,h)&=\frac{1}{j}\sum_m m\int\frac{d\omega}{\pi}f(\omega)\rho_m(\omega,T,h)\\&=\frac{1}{jZ_{4f}(T,h)}\sum_m m\int\frac{d\omega}{\pi}e^{-\beta\omega}A_m(\omega,T,h)\ .\end{aligned} \tag{2.18}$$

These are not the only contributions to the electron number and polarization linear in the impurity number: there also arise terms involving the polarization of the conduction electrons about the impurity. However, these terms are small in the extreme Kondo limit of interest in this paper[51] and thus Eqs. (2.17) and (2.18) are the expressions of interest for evaluating the field-dependent occupancies and polarization.

The other physical response function of interest is the susceptibility. The full dynamical susceptibility $\chi_D(z,T)$ is given, in the spirit of Eqs. (2.12–2.14) above, by

$$\begin{aligned}\chi_D(z,T)=&\frac{(g_j\mu_B)^2}{Z_{4f}(T)}\\&\times\sum_m m^2\int\frac{d\omega}{\pi}e^{-\beta\omega}A_m(\omega,T)\\&\qquad\times[g_m(\omega+z,T)+g_m(\omega-z,T)]\ .\end{aligned} \tag{2.19}$$

The resulting expression for the static susceptibility is given by

$$\begin{aligned}\chi(T)=&\frac{-2(g_j\mu_B)^2}{Z_{4f}(T)}\\&\times\sum_m m^2\int\frac{d\omega}{\pi}e^{-\beta\omega}A_m(\omega,T)\,\mathrm{Reg}_m(\omega,T)\ .\end{aligned} \tag{2.20}$$

As per Eqs. (2.17) and (2.18) the above equation neglects effects due to polarization of the conduction electrons about the impurity site, which is valid in the extreme Kondo limit. At low temperature, the static susceptibility tends to a limiting constant value. I can define a temperature scale $T_L$ after Rasul and Hewson[19] by the formula

$$\chi(0)=\frac{(g_j\mu_B)^2j(j+1)}{3k_BT_L} \tag{2.21}$$

and it of course is true that $T_L$ is essentially the Kondo temperature, namely,

$$T_L\sim D\left[\frac{\Gamma}{\pi|\epsilon_f|}\right]^{1/N_{\mathrm{grd}}}\exp\left[-\frac{\pi|\epsilon_f|}{N_{\mathrm{grd}}\Gamma}\right]\ . \tag{2.22}$$

The expression on the right-hand side of the above equation is precisely the quantity $T_0$ utilized in our previous work.[12] For the purposes of computing the quantities of this paper, $T_L$ is a more suitable energy scale, and moreover a well-defined prescription exists for identifying it for all values of $N_{\mathrm{grd}}$. $T_0$ defined as the peak position of the "Kondo" resonance for $T\to 0$ in our previous work, has a problematic definition for $N_{\mathrm{grd}}=2$ for which the resonance is pulled off the fermi level only to the extent that the occupancy $n_f(T)$ differs from unity.

However, while $T_L$ is a natural quantity, for spin $\frac{1}{2}$ the more commonly encountered quantity is $T_K$, the energy scale identified from renormalized high-temperature perturbation theory.[16] I have used both $T_L$ and $T_K$ use for reporting spin-$\frac{1}{2}$ results. The relation between $T_L$ and $T_K$, first obtained by Wilson,[14] and later elucidated in the

context of Bethe-ansatz solutions by Andrei and Lowenstein[53] and Rasul and Hewson,[19] is that $T_L(j=\frac{1}{2})=2.438T_K(j=\frac{1}{2})$. I apologize to the reader for the plethora of energy scales; comfort may be taken in the fact that the "Wilson numbers" relating $T_L$ and $T_K$ are pure numbers depending only upon the degeneracy.

## III. NUMERICAL RESULTS FOR OCCUPANCY AND POLARIZATION

### A. Numerical details

The solution of the integral equations was performed iteratively, with the pseudofermion spectra placed on separate logarithmic meshes extending from $-30D$ to the peak of the fermion spectral function, and from the peak of the fermion spectral function to $30D$. Similarly, the two pseudoboson meshes ran from $-30D$ to the peak of the pseudoboson spectral function and from the peak of the pseudoboson spectral function to $30D$. A total of 83 mesh points were used for each spectra. On a VAX-11/780 computer, a typical self-consistent evaluation of pseudoboson and pseudofermion spectra for a given set of model parameters, at one value of temperature and magnetic field took about 4 cpu minutes for degeneracy 2, and 12 cpu minutes for degeneracy 6.

While the meshes described above were adequate for computing the moments which feed into calculations of the occupancy and magnetization, they were not sufficiently accurate to convolute for the calculation of spectra, except at zero frequency. A corollary is that they did not allow precise calculations to very low temperatures as were obtainable with the much larger meshes used in previous works. For example, for the $j=\frac{5}{2}$ calculation, the lowest obtainable temperature with 603 points was about $\frac{1}{70}$ of $T_L$, while for 83 points severe numerical instabilities began to set below about $0.18T_L$. Because the lowest Zeeman level tends to a delta function in the high field limit, I also had difficulty pushing the calculations to very high fields.

The sum rules for the spectral functions (that they integrate to unity) were checked always, and typically these relations held to a tenth of a percent or so. In the case of the spin-$\frac{5}{2}$ run, additional checks were provided at zero field by comparing to susceptibilities and occupancies computed with more precise 603 point meshes. The agreement was good to about 2%. Another comparison for calibration purposes is made clear in Fig. 1, where the limited calculation of $\chi(T)$ for spin $\frac{1}{2}$ is compared with the exact results obtained by numerical renormalization-group and Bethe-ansatz calculations. This illustrates the surprising result that this nominal large degeneracy calculation works quite well for spin $\frac{1}{2}$, as has been noted before.[22,23]

Parameter choices were motivated by the desire to reach the universal regime where $T_K/D$ is small so that conduction-band polarization effects are small. However, the parameters were also chosen so as to give a large enough $T_K$ so that numerical results in the non-trivial regime below $T_K$ were obtainable. Moreover, the hybridization widths $\Gamma$ were chosen to be consistent with the normalization of the large degeneracy limit; namely $N_{\rm grd}\Gamma$ is held constant while $N_{\rm grd}$ is increased. For all calculations reported here, $\epsilon_f=-0.152D$ and $N_{\rm grd}\Gamma=0.0954D$. The values of the Kondo energy scale are $T_K(j=\frac{1}{2})=4.37\times10^{-4}D$ and $T_L(j=\frac{5}{2})=3.28\times10^{-3}D$.

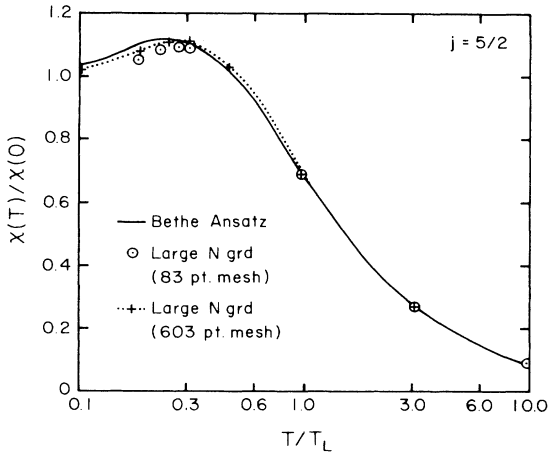


FIG. 1. Reduced susceptibility vs temperature for $j=\frac{1}{2}$. $T$ is measured in units of $T_L$ defined in Eq. (2.20). Note the good agreement of the circles calculated from self-consistent large degeneracy theory and the exact Bethe-ansatz results (Ref. 82) noted previously for large $N_{\rm grd}$ theories (Refs. 22 and 23).

### B. Occupancy

The occupancies of the various Zeeman levels as a function of applied field at the lowest calculated temperatures are plotted in Figs. 3 ($j=\frac{1}{2}$) and 4 ($j=\frac{5}{2}$).

Clearly, the total $j=\frac{1}{2}$ occupancy varies rather little as a function of field despite the strong field dependence of the individual Zeeman level occupancies. There are two reasons for this. First the Kondo resonance for spin $\frac{1}{2}$ is very close to a particle-hole symmetric shape as can be reckoned from the Friedel sum rule[54] which puts the resonance right on the Fermi level for unit occupancy and degeneracy 2. Hence, this would tend to freeze the occupancy. The other reason is that the charge fluctuations present in this asymmetric Anderson Hamiltonian which break particle-hole symmetry are expected to be reduced dramatically only on energy scales of order $\Gamma$ where the deep $f$ level near $\epsilon_f$ begins to Zeeman split. As $\Gamma$ is some 2 orders of magnitude above $T_K$ for these calculations here, we cannot expect to see any reasonable change in $n_f(T,h)$ for the low fields presented in Fig. 3. Note also that the contribution to $n_f(T,h)$ from charge fluctuations is expected to be of order $\Gamma/|\pi\epsilon_f|$ which is about 0.1 for these parameters. Thus, for a starting occupancy of 0.86, there is little room for variation of $n_f(T)$ as a function of field.

The total occupancy of the $j=\frac{5}{2}$ level shows far more field dependence than that of $j=\frac{1}{2}$ because the Friedel sum rule constraint now forces the resonance to reside away from the Fermi level near $T_L$ with width of order $\pi T_L/6$ so as to satisfy $\delta(E_{\rm Fermi})$ approximately equal to

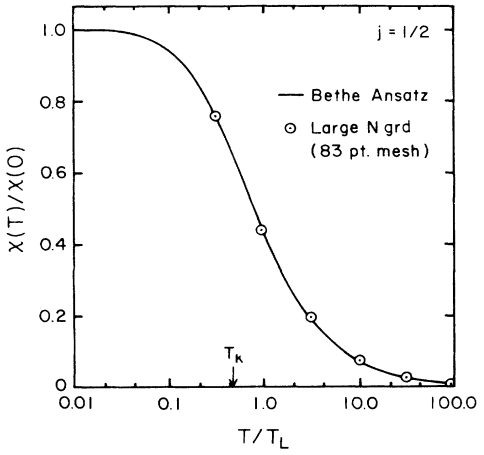


FIG. 2. Reduced susceptibility vs temperature for $j=\frac{5}{2}$. As per Fig. 1, agreement with Bethe ansatz results (Ref. 18) are excellent, though systematic discrepancies are visible below $T_l$ where $\chi(T)$ peaks. In particular, the coarser 83 point mesh used in this work shows systematic deviation from the 603 point mesh used in previous work (Ref. 9).

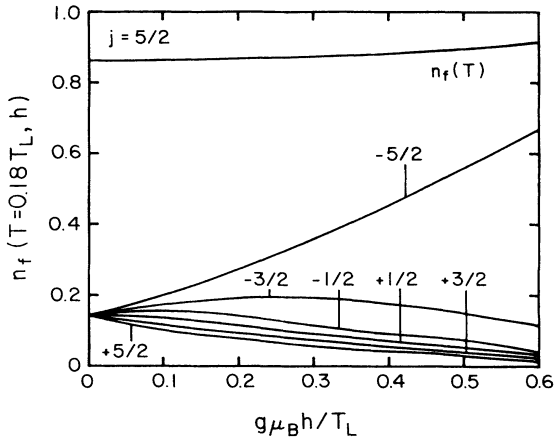


FIG. 4. Occupancy vs magnetic field for $j=\frac{5}{2}$. As with $j=\frac{1}{2}$ the rise to saturation of the lowest Zeeman level follows initial linear changes with field. Note the nonmonotonicity of the occupancy for the two next to lowest levels.

the width divided by the position which is approximately $\pi/N_{\rm grd}$. The latter near equalities are valid, of course, only in the limit of large $N_{\rm grd}$. Moreover, as $\Gamma$ is smaller by a factor of 3 than for $j=\frac{1}{2}$ with the parameter choices here, most of the low-field deviation of the occupancy from unity is arising from the Kondo resonance. Explicitly, the contribution from charge fluctuations is about 0.03 here.

The occupancies of the individual Zeeman levels mimic those of the free ion in the broad sense that the initial linearities are followed by subsequent saturation of the lowest-lying Zeeman singlet. In more detail, the nonmonotonic behavior of the $m_z=\frac{3}{2},\frac{1}{2}$ levels for $j=\frac{5}{2}$ is also found in the free ion. The important difference, of course is the far less rapid saturation of the curves in Figs. 3 and 4 than the corresponding free-ion curves, with e.g.,

$$n_f(T,h\rangle\rangle T_K)-n_f(-\tfrac{1}{2},T,h\rangle\rangle T_K)\sim 1/|\ln(h/T_K)|$$

for $j=\frac{1}{2}$,[55] as compared to exponential saturation for the free ion. This logarithmic saturation is of course also slower than the algebraic ($\sim 1/h$) saturation which arises in a simple resonant level model.

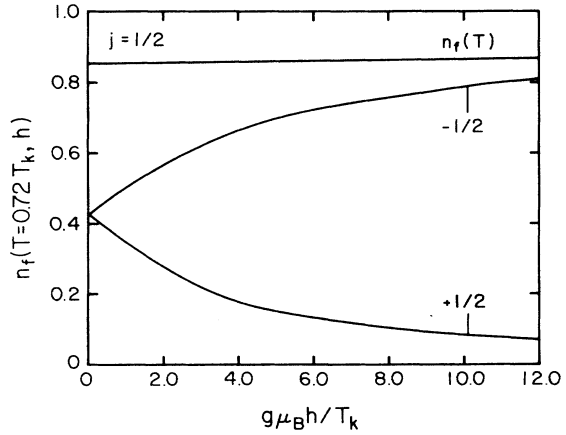


FIG. 3. Occupancy vs magnetic field for $j=\frac{1}{2}$. Qualitatively, this shows the expected behavior of initial linear changes followed by subsequent saturation of the lower Zeeman level to $n_f(T)$.

### C. Polarization

The polarization curves for $j=\frac{1}{2}$ and $j=\frac{5}{2}$ are presented in Figs. 5 and 6, respectively. For comparison, zero-temperature Bethe-ansatz curves[19] are plotted as dashed

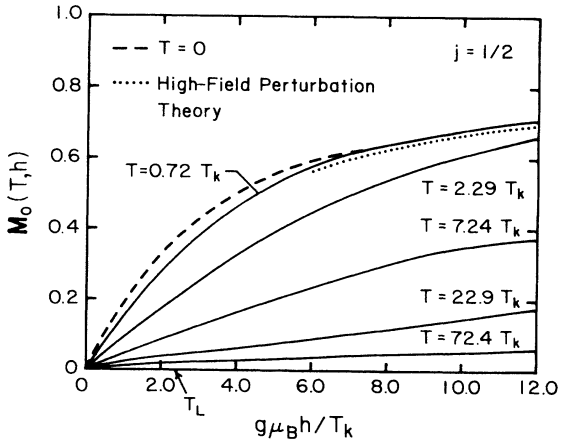


FIG. 5. Polarization vs field for $j=\frac{1}{2}$. The polarization is defined as the magnetization divided by its high-field saturation value. Note the apparent approach towards the exact zero-temperature Bethe-ansatz result (Ref. 19), and the good agreement with high-field perturbation theory. Note, however, that the present calculation systematically overestimates the high-field perturbation theory result. See also Table I.

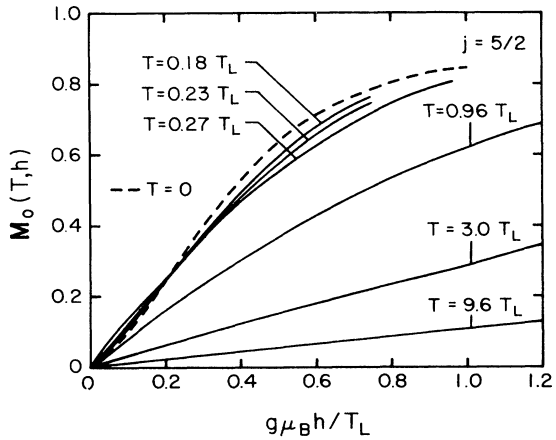


FIG. 6. Polarization vs field for $j=\frac{5}{2}$. Note the appearance of an inflection point in contrast to the curves of Fig. 5; for more details, see Fig. 7. Again the low-temperature curves appear to be approaching the low-temperature Bethe-ansatz result (Ref. 19). See also Table II.

lines, and the zero-temperature high-field perturbation theory results as dotted lines. The lowest-temperature curves appear to be saturating to the exact results which offers further evidence of the success of the self-consistent large degeneracy approach for calculating properties of the Anderson model. Tables I and II contain comparison of finite temperature calculations between the large-$N_{\rm grd}$ approach and Bethe-ansatz approach. As can be seen, the agreement is good though the self-consistent approach appears to overestimate the exact values for high $h/T$. This is as likely to be a numerical artifact as a real one, since the high field numerics is difficult to stabilize.

TABLE I. Comparison of polarization obtained by Bethe-ansatz and large-$N_{\rm grd}$ approaches for $N_{\rm grd}=2$. The Bethe-ansatz results (for the spin-$\frac{1}{2}$ Kondo model) are taken from Ref. 16, Fig. 16. The large $N_{\rm grd}$ results have been read off the curves of Fig. 5. As these themselves are interpolated curves, I place an upper bound of 5% on combined graphical sighting-interpolation errors. Figure 2 suggests that there is at most a 2% numerical error from the utilization of a coarse mesh. Hence, one should consider discrepancies between Bethe ansatz and large $N_{\rm grd}$ results as very significant from the level of 7% and higher. Clearly, the agreement is reasonably good, although systematic overestimates are clear for high $h/T$. I cannot rule out the possibility that this is numerical in origin, since convergence of high field numerics is more delicate.

| $g\mu_B h/k_B T_K=1.19$ $g\mu_B h/k_B T$ | $\mathbf{M}_0(T,h)$ $1/N_{\rm grd}$ | $\mathbf{M}_0(T,h)$ Bethe ansatz |
|---|---|---|
| 0.016 | 0.01 | 0.01 |
| 0.05 | 0.02 | 0.02 |
| 0.16 | 0.05 | 0.05 |
| 0.52 | 0.10 | 0.10 |
| 1.63 | 0.18 | 0.16 |
| $g\mu_B h/k_B T_K=2.38$ $g\mu_B h/k_B T$ | $\mathbf{M}_0(T,h)$ $1/N_{\rm grd}$ | $\mathbf{M}_0(T,h)$ Bethe ansatz |
| 0.03 | 0.01 | 0.01 |
| 0.10 | 0.03 | 0.03 |
| 0.33 | 0.09 | 0.09 |
| 1.04 | 0.21 | 0.20 |
| 3.31 | 0.32 | 0.27 |

TABLE II. Comparison of polarization obtained by Bethe-ansatz and large-$N_{\rm grd}$ approach for $N_{\rm grd}=6$. Bethe-ansatz results for the Coqblin-Schrieffer model are taken from Ref. 10. As per Table I, the accuracy with which these results are to be compared is at about the 7% level. Clearly, as for Table I, agreement is good apart from systematic over estimation by the large-$N_{\rm grd}$ approach at high values of $h/T$.

| $g\mu_B h/k_B T_L=0.2$ $g\mu_B h/k_B T$ | $2.5\mathbf{M}_0(h,T)$ $1/N_{\rm grd}$ | $2.5\mathbf{M}_0(h,T)$ Bethe ansatz |
|---|---|---|
| 0.021 | 0.06 | 0.07 |
| 0.067 | 0.16 | 0.18 |
| 0.21 | 0.41 | 0.43 |
| 0.74 | 0.63 | 0.61 |
| 0.87 | 0.63 | 0.61 |
| 1.11 | 0.63 | 0.59 |
| $g\mu_B h/k_B T_L=0.5$ $g\mu_B h/k_B T$ | $2.5\mathbf{M}_0(h,T)$ $1/N_{\rm grd}$ | $2.5\mathbf{M}_0(h,T)$ Bethe ansatz |
| 0.052 | 0.16 | 0.14 |
| 0.17 | 0.38 | 0.40 |
| 0.52 | 0.91 | 0.93 |
| 1.85 | 1.38 | 1.32 |
| 2.17 | 1.44 | 1.36 |
| 2.78 | 1.50 | 1.39 |

The finite-temperature magnetization curves for the $j=\frac{1}{2}$ model have been computed before by the Bethe-ansatz approach and so our curves do little more than establish their tractibility within this approach. The behavior as a function of field and temperature is purely monotonic. Of greater interest are the curves for $j=\frac{5}{2}$, for which clear nonmonotonicity as a function of field and temperature is evident. While the nonmonotonicity is somewhat difficult to see in Fig. 6, it is readily evident in Figs. 1 and 7, the latter of which, in a sense, plots a measure of the finite-field susceptibility.

The peak in $\chi(T,0)$ and the "superlinear" polarization have a common origin in the fact that the Kondo resonance resides away from the Fermi level for high degeneracy. The susceptibility, after all, serves as a rather coarse-grain spectroscopy of the electronic density of states. Hence, until the magnetic field becomes comparable to the resonance position ($\sim T_L$), the lowest Zeeman level does not begin to dominate. The inflection point in $\mathbf{M}_0(T,h)$ vanishes at precisely the temperature where the static susceptibility is maximum. Topologically, this is plausible, since the simplest possibility given a maximum of $\chi(T,h)$ in the $(T,h)$ plane along both axes is that there be a monotonic interpolation between the two. Thus at fixed $T$, one would not expect to encounter a maximum beyond the point where $\chi(T,0)$ is peaked. The nonmonotonicity is marginal at $N_{\rm grd}=3$ as pointed out first by Rasul and Hewson,[19] and elucidated in the mean-field

treatment of Read and Newns.[56] The nonmonotonicity has been observed in some compounds, most notably YbCuAl,[57,58] although it should be noted that crystal-field effects can also produce significant nonmonotonicity in $\chi(T,h)$.[59] Within the simple molecular field model presented in the next section it is shown that the particular nonmonotonicity pointed out here can have interesting consequences for magnetic ordering.

## IV. MOLECULAR FIELD THEORY

### A. Molecular field model and calculation of phase diagrams

In this section I present a simple molecular field theory for the Anderson lattice model. The basic ideas for the calculations presented here are as follows.

(i) The free energy of the Anderson lattice can be rigorously written in a way which allows expansion in powers of the intersite interaction. The zeroth-order free energy in this expansion is an incoherent array of Kondo-Anderson impurities. Hence, this zeroth-order picture is precisely that taken in the "Kondo-volume collapse" calculations.[60]

(ii) Of the remaining intersite terms, there are those which correspond to multisite (three and higher) exchange processes between the $f$ electrons and those which correspond to simple two-site RKKY charge and spin interactions between sites. The former give the coherent modifications to the two particle pseudofermion Green's functions. I shall consider only the simplest intersite exchange interaction between $4f$ moments

(iii) The intersite exchange is then treated within the molecular field approximation, and thus the model free energy used here has the form (per site) for ferromagnetic RKKY coupling ($\lambda>0$)

$$F(T,\mathbf{M})=-k_B \ln Z_f(T,\lambda M)+\tfrac{1}{2}j\lambda M^2 , \tag{4.1}$$

where $j$ is the Hund's rule ground angular momentum of the moment bearing configuration, $\mathbf{M}$ is the polarization (normalized to unity at saturation), and $Z_f$ is the single-site Anderson model partition function at temperature $T$ and effective magnetic field $\lambda\mathbf{M}$. In Eq. (4.1), polarization of the conduction band is neglected, which is valid to order 1 bandwidth.[51] Generalization of (4.1) to antiferromagnetic order is straightforward as it is in the case of pure local moments. With the molecular field defined as per Eq. (4.1), the local moment paramagnetic Curie-Weiss temperature is $(j+1)\lambda/3$ in the absence of any hybridization.

(iv) Finally, extremization of (4.1) with respect to $\mathbf{M}$ yields the molecular field equation

$$\mathbf{M}=\mathbf{M}_0(T,\lambda\mathbf{M}) , \tag{4.2}$$

where $\mathbf{M}_0$ is the single site polarization derived from $Z_f$. Solution of (4.2) yields values of the spontaneous polarization and critical temperatures.

In Fig. 8, contours of constant polarization are plotted in the $\lambda$-$T$ plane for $N_{\rm grd}=2$. The critical boundary is defined by $\mathbf{M}=0$. $\lambda$ is measured in units of $T_L$. For

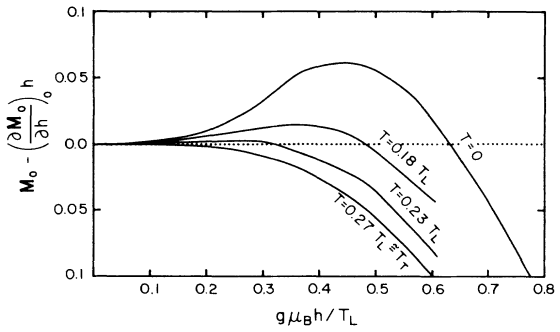


FIG. 7. Deviation of one-site polarization from linearity for $j=\frac{5}{2}$. The important feature here is that as $T$ approaches $T_t$, the temperature where $\chi(T)$ peaks, the low-field curvature of the polarization approaches zero, becoming positive for $T>T_t=0.28T_L$. This behavior is expected to occur for $j>1$. The zero-temperature result is the Bethe-ansatz curve (Ref. 19).

$T=0$, $(j+1)\lambda/3T_L=1$ is the boundary to the left of which magnetic ordering cannot occur. This result is analagous to the Stoner criterion for itinerant magnets since $1/T_L$ is roughly the quasiparticle density of states at the Fermi level. As $(j+1)\lambda/3T_L\to 1+\epsilon$, both transition temperature and spontaneous magnetization vanish as $\epsilon^{1/2}$. For high $\lambda/T_L$, $\mathbf{M}(T=0)$ and $3T_c/(j+1)\lambda$ approach unity, although only like $\sim 1-A/\ln\lambda$ in either case.

At this stage it is worth noting that previous calculations along these lines have been performed with $\mathbf{M}_0$ in (2) modeled by that of a fermion resonant level straddling the fermi level with $N_{\rm grd}=2$.[36,37] The Lorentzian resonance possesses width $\Gamma$ assumed to be of order $T_L$. For small $\lambda/\Gamma$, the results presented here are qualitatively identical to those of the previous studies; quantitative discrepancies persist for all $\lambda$, and in particular, the logarithmic behavior valid for large $\lambda/T_L$ cannot come out of the resonant level model. There is also a nontrivial resonance narrowing effect which is missed in the simple resonance model. The previous studies went beyond this current one in the consideration of more sophisticated magnetically ordered structures upon inclusion of anisotropy, which in the interest of simplicity, have been neglected here.

Next, consider the high-degeneracy case, specifically, $j=\frac{5}{2}$. There is a pronounced difference between this case and the spin-$\frac{1}{2}$ problem. In accordance with the Friedel sum rule, the Kondo resonance peaks off the fermi level for degeneracies greater than 2.[54] The excitation to the moment bearing configuration is thus inelastic and highly damped. The clearest manifestations of this effect in single site properties are (i) finite temperature maxima in the static susceptibility and linear specific heat coefficient,[61,62] (ii) a non-Lorentzian line shape in the dynamic spin excitation spectrum,[11,13] (iii) and an inflection point in the magnetization as a function of field (i.e., a nonzero maximum in the differential susceptibility)[19] As illustrated in Fig. 7, the magnetization inflection goes away as the temperature is raised, vanishing precisely at the temperature

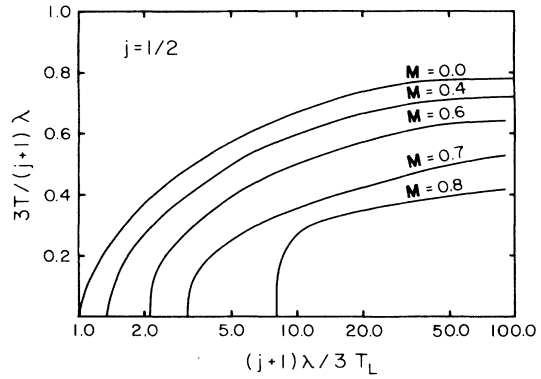


FIG. 8. Contours of constant saturation polarization for the spin-$\frac{1}{2}$ Anderson lattice within molecular field theory. The molecular field constant $\lambda$ is defined so that $\lambda\mathbf{M}=g\mu_B h_{\rm mol}$. $T_c$ and $\mathbf{M}(0)$ vanish as $[(j+1)(\lambda/3T_L-1)]^{1/2}$ for $(j+1)\lambda/3T_L$ tending to unity, and the saturation to local moment behavior $[3T_c/(j+1)\lambda=1$ and $\mathbf{M}(0)=1]$ occurs logarithmically. Note that $\mathbf{M}$ can represent the staggered polarization for nearest-neighbor antiferromagnetic coupling.

$T_t$ where $\chi(T)$ peaks.

The magnetization inflection has immediate consequences for the molecular field theory, as evidenced in the constant polarization plots for $j=\frac{5}{2}$ shown in Fig. 9. For low enough values of $\lambda$, there are three solutions to (4.2) below $T_t$, two of which are stable. A Maxwell construction must then be used to determine the shape of the magnetization curve as a function of field and to determine which state (polarized or paramagnetic) has the lowest free energy in the absence of field. The first-order phase boundary between magnetic and paramagnetic states in zero applied field appears as the dashed line in Fig. 9. For $\lambda>0$, applied field can stabilize the magnetic state for $\lambda>j\mu_{\rm eff}^2/3\chi_I$, where $\chi_I$ is the differential susceptibility at the inflection point. This criterion defines the phase boundary between the applied field "metamagnetic" state and the zero-field paramagnetic tate.

Hence, the topology of the magnetization in the field-temperature plane for high degeneracy generates a tricritical point within this simple molecular field calculation. Otherwise, the discussion of $\mathbf{M}$ and $T_c$ as a function of $\lambda/T_L$ goes through as in the spin-$\frac{1}{2}$ case.

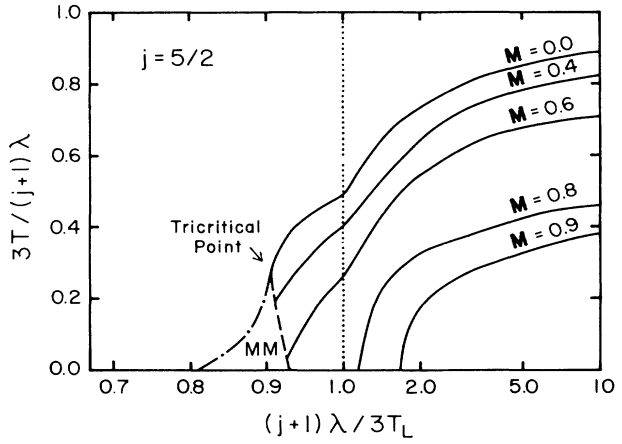


FIG. 9. Contours of constant polarization for the $j=\frac{5}{2}$ Kondo lattice within the molecular field approximation. As for $j=\frac{1}{2}$, the approach to local moment behavior is logarithmic; however, factors of the inverse degeneracy increase the rapidity of this saturation. The new feature of these curves is the existence of a discontinuous drop of $\mathbf{M}$ to zero along the dashed line. For ferromagnetic coupling, this defines the metamagnetic ferromagnetic phase boundary. The dotted-dashed metamagnetic-paramagnetic boundary (to the left of which field induced first-order polarization jumps are no longer possible) is determined from the slope of the one-site polarization at the inflection point. Since the zero-field first-order line joins to a line of second-order transitions at $T_t$, this is to be identified with a tricritical point in the $T,\lambda$ plane. The lowest possible $\mathbf{M}(0)$ value is approximately equal to 0.65. Such tricritical behavior is expected to occur for all $j>1$ (see Fig. 7).

### B. Additional theoretical details

Before discussing possible experimental implications of this study, it is worth noting some further results.

(i) In the ferromagnetic case, the effective Curie moment $\mu^2(T_c^\dagger)$ defined by

$$\mu^2(T_c^\dagger)=\lim_{T\to T_c^\dagger} 3\chi(T)(T-T_c) \tag{4.3}$$

has anomalous behavior as seen in Fig. 10. For $j=\frac{1}{2}$ and $T_c/T_L$ tending to zero, $\mu_{\rm eff}^2/\mu^2(T_c)$ vanishes linearly with $T_c$, while it overshoots the local moment limit of 1 for $T_c/T_L\sim 0.1$, finally settling to unity for $T_c\gg T_L$. Similar behavior is seen for $j=\frac{5}{2}$, except that $\mu^2$ vanishes at the critical point $T_t$.

(ii) Volume effects can modify $T_c$ significantly. It is relatively easy to see how $T_c$ will change with pressure. Define $\tilde{\chi}(T)=3\chi(T)/\mu_{\rm eff}^2$. Denote the pressure (relative to

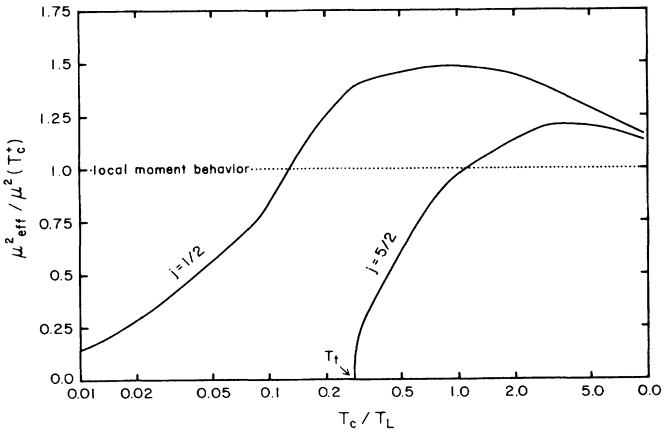


FIG. 10. Inverse Curie-Weiss law moment vs temperature. The moment is determined from $\lim_{T\to T_c^\dagger} 3(T-T_c)\chi(T)=\mu^2(T_c)$. This vanishes linearly in $T_c$ for $T_c\to 0$ and $j=\frac{1}{2}$, and linearly in $T_c-T_t$ for $T_c\to T_t$ for $j=\frac{5}{2}$. The overshoot of local moment behavior is due to the logarithmic behavior of $\chi(T)$ for high $T$, e.g., to leading logarithmic behavior for $j=\frac{1}{2}$, $\mu_{\rm eff}^2/\mu^2(T_c)\approx 1+[\ln(2.4T/T_L)]^{-1}$ when $T\gg T_L$.

ambient pressure) by $P$, the bulk modulus by $B$, and the ambient volume $V_0$. Introduce Grüneisen parameters $\gamma_\chi(T)$ (for $\chi$) and $\gamma_\lambda$ (for $\lambda$) according to the general definition

$$\gamma_0 = \frac{\partial \ln O}{\partial \ln V} . \tag{4.4}$$

Then near ambient pressure, the equation for $T_c$ is

$$\frac{j+1}{3}\lambda\tilde{\chi}(T_c) = 1 + \frac{P}{BV_0}[\gamma_\lambda + \gamma_\chi(T_c)] . \tag{4.5}$$

Immediately, one can solve for the initial change of $T_c$ with pressure which is given by

$$\frac{\partial \ln T_c}{\partial P} = \frac{\gamma_\lambda + \gamma_\chi(T_c)}{BV_0 \,|\, \partial \ln \chi(T)/\partial \ln T \,|_{T_c}} . \tag{4.6}$$

Note that $\chi(T) = \chi(0) f(T/T_L)$, where $f(x)$ is a universal function. Introducing the Grüneisen parameter $\gamma_{T_L}$, then it is clear that

$$\gamma_\chi(T) = -\gamma_{T_L}\left[1 + \frac{\partial \ln f(T/T_L)}{\partial \ln T}\right] . \tag{4.7}$$

Specializing to spin $\frac{1}{2}$ I note that

$$\frac{\partial \ln \chi(T)}{\partial \ln T} \approx -2\tilde{\alpha}\left[\frac{T}{T_L}\right]^2, \quad T \ll T_L$$
$$\approx -\left[1 - \frac{\alpha}{\ln^2(\eta T/T_L)}\right], \quad T \gg T_L \tag{4.8}$$

where $\alpha$, $\tilde{\alpha}$, and $\eta$ are positive pure numbers of order unity. Thus, for sufficiently high temperatures, the behavior of the intersite exchange dominates the pressure dependence, while for sufficiently low temperatures the behavior of the susceptibility dominates. Note that $\gamma_{T_L}$ and $\gamma_\lambda$ are both related to the change of the effective (Coqblin-Schrieffer) exchange integral. If one assumes that the volume dependence of each parameter enters through the volume dependence of $g = |N(0)J_{CS}| = N_{grd}\Gamma/\pi|\epsilon_f|$, then $\gamma_\lambda \approx 2\gamma_g$, and $\gamma_{T_L} \approx \gamma_g/g$. Further, $\gamma_g = \gamma_\Gamma - \gamma_{\epsilon_f}$. In Ce compounds, the value of the $f$-level position is little sensitive to compression[63] while the hybridization can have dramatic sensitivity. For the purposes of understanding the $\gamma$-Ce to $\alpha$-Ce volume collapse in terms of the Anderson model, $\gamma_{T_L}$ was taken to be of order $-40$ or so.[60] On the other hand, in the Yb compounds there are theoretical[63] and experimental[64] reasons to believe that $\gamma_{\epsilon_f}$ dominates which would make $\gamma_g$ *positive*. The limiting forms (high and low temperature) for the pressure derivative of $T_c$ are

$$\frac{\partial \ln T_c}{\partial P} \approx \frac{1}{BV_0}\left[|\gamma_\lambda| - |\gamma_{T_L}| \frac{\alpha}{\ln^2(\eta T_c/T_L)}\right], \quad T_c \gg T_L$$
$$\approx -\frac{1}{2\tilde{\alpha}BV_0}\left[\frac{T_c}{T_L}\right]^2 |\gamma_{T_L}|, \quad T_c \ll T_L . \tag{4.9}$$

If $\gamma_g$ is negative (as for Ce compounds), Eqs. (4.9) lead one to expect a positive slope (enhanced $T_c$) at high $T$ and a negative slope (suppression of $T_c$) at low $T$. If $\gamma_g$ is positive (as it may well be for Yb compounds) then one expects $T_c$ enhancement at low $T$ and $T_c$ suppression at high $T$.

(iii) As pointed out previously[36] in terms of the resonant level model, the specific heat may still possess a sizeable linear term in the presence of ordering. Within that work and the current one, the linear coefficient at $T=0$ is simply that of the single site in the presence of a magnetic field equal to the exchange field. Physically, the Zeeman split Kondo resonances still will have some spectral weight at the Fermi level. Hence, one need not interpret residual linear specific-heat terms in terms of itinerant magnetism with a partially gapped Fermi surface, as had been the case, for example, with $U_2Zn_{17}$.[42]

(iv) The specific heat within the mean-field theory shows interesting behavior as the tricritical point (for large degeneracy) is approached from above. Within Landau theory it is easy to show that the specific-heat jump at $T_c$ is given by

$$\Delta C_p \sim \frac{3j}{2(j+1)b_4(T_c)}\left[\left|\frac{\partial\tilde{\chi}(T)}{\partial T}\right|_{T_c}\right]^2 , \tag{4.10}$$

where $b_4(T)$ is the coefficient of the quartic term (in the polarization) of the free energy.[65] Since $\chi(T_t)$ is a maximum and since $b_4(T)$ vanishes linearly at $T_t$, then $\Delta C_p \sim (T_c - T_t)$ and thus the jump vanishes linearly on approaching $T_t$. Obviously, the relevance of such behavior may be mitigated in any more sophisticated treatment which goes beyond molecular field theory.

(v) While it may seem troubling that one is making a transition to a paramagnetic state and thus a more "disordered" state, in fact the entropy of this paramagnetic phase is diminishing since the Kondo state is a singlet, and thus there is no paradox.[66]

### C. Possible experimental relevance

The most interesting aspect of this work is perhaps the prediction of novel tricritical behavior for high-degeneracy systems. This behavior depends primarily upon the presence of the inflection point in the magnetization curve present for $N_{grd} > 3$, and thus may be a feature which transcends the simple assumptions made in these calculations.

It is not outside the realm of possibility that via alloying (chemical pressure) or application of physical pressure that magnetic ordering might be introduced in YbCuAl where such an inflection point has been seen. This reasoning is based on the analysis of the pressure dependence of $T_c$ in Sec. IV B and the thought that pressure decreases $T_L$ for Yb, assuming that the $4f^{13}$ configuration is nominally stable, and that the Wigner-Seitz radius is larger than 2 Bohr radii.[63] However, a problem is that the requirement of a relatively low Kondo temperature will tend to drive the system into a region where crystal-field energies become comparable to or larger than the Kondo temperature, and thus the ground state will be characterized by a lower-degeneracy Anderson model[27] which will likely not possess tricritical behavior.

Therefore perhaps the most encouraging possibilities are

magnetically ordered Eu compounds, particularly $EuRh_3B_2$, which orders ferromagnetically.[34,35] The reason is that the moment bearing configuration for Eu is the $4f^7$ which has pure spin $j=\frac{7}{2}$ ground state. Not only is high degeneracy guaranteed when the Kondo temperature is high, but also as the Kondo temperature is lowered since crystal-field splittings are miniscule in such pure spin cases (the crystal field coupling through the orbital degrees of freedom).

If this picture is at all relevant for $EuRh_3B_2$ it would appear to possess a low Kondo temperature on the basis of its high ordering temperature and nearly full saturation moment, and thus it would seem to be a natural choice for alloying experiments or pressure work. The experimental requirement is that the Kondo temperature be driven up in this case. If isostructural $CeRh_3B_2$ (Ref. 41) can serve as a guide, alloying Ru on the Rh sites or applying direct pressure should do the job. In that case although the analysis of the previous section suggests $T_c$ will likely go up with the application of pressure, one can nevertheless expect a significant reduction of the low temperature saturation moment due to the tendency to *suppress* magnetism at low temperatures. If on the other hand, Eu behaves like Yb, and $\gamma_g$ is positive, then one needs to alloy to provide "negative pressure" so as to suppress the low-temperature magnetism. A possible complication with the alloying experiment is that $EuRu_3B_2$ does not form.[67]

## V. SUMMARY

In summary, I have applied the self-consistent large orbital degeneracy theory for the degenerate Anderson model to calculations of the magnetization and occupancy as functions of magnetic field and temperature. The magnetization results agree well with exact Bethe-ansatz results, although there are some systematic discrepancies detectable. A simple application of the results is made within molecular field theory for the Anderson lattice, which is expected to be valid in the extreme Kondo regime provided the itinerant character of the $f$ electrons is small and there are no multisite Kondo effects. Within this simple molecular field theory, no magnetic order is possible if the intersite interaction is smaller than the characteristic Kondo energy scale, and any ordering will show reduced moment strength reminiscent of itinerant magnetism. For high orbital degeneracy ($N_{\rm grd}>3$), novel tricritical behavior sets due to the intrinsic feature that the Kondo resonance sits away from the Fermi level. I propose that such behavior might be observable in allowing or pressure experiments on $EuRh_3B_2$ and YbCuAl. Since the calculations exclude coherent modifications of the heavy-electron state requisite for a discussion of charge density wave, superconducting, spin density waves, or any other collective phenomena specific to a periodic electron gas, no discussion of these phenomena is possible within the theory presented here.

## ACKNOWLEDGMENTS

I have benifited from discussions with L. J. Sham, K. Yang, J. W. Wilkins, R. M. Martin, J. W. Allen, S. Lambert, M. B. Maple, N. E. Bickers, N. Read, A. Ruckenstein, M. Thorpe, and T. Kaplan. This research was supported by the National Science Foundation under Grant No. DMR85-14195. I am grateful for the hospitality of the Institute of Theoretical Physics where some of this manuscript was prepared, and for partial support through National Science Foundation Grant No. PHY82-17853 supplemented by funds from the National Aeronautics and Space Administration.

## APPENDIX A

In this appendix, formal justification is given for the molecular field equations (4.1) and (4.2). The derivation clearly demonstrates the restricted regime for which one might expect the equation to be applicable. The restrictions are summarized as follows. (1) One must be in the extreme Kondo regime ($T_L/\Gamma \ll 1$) so that (a) chemical potential effects due to the $f$ electrons are weak,[68] (b) well-defined local moments exist at high temperature, and (c) the strongly energy-dependent terms in the simplest perturbative estimate of the effective intersite interaction function are small. (2) One must neglect $n$-site exchange processes between $f$ moments with $n>2$. These processes will be seen to feed into the coherent modification of the two-site exchange processes. (3) One must neglect repeated scattering of two-site exchange processes (and thereby the possibility of multisite Kondo effects[69,70]). Within the approximations specified by (1)–(3), one further neglects the dynamics of the simplest two-site exchange processes. As this corresponds to treating the normal RKKY interactions as static, it is probably a reasonable approximation. The extent to which the normal RKKY interactions dominate the perturbatively evaluated two-site interaction is the subject of Appendix B.

The plan of this appendix is as follows. First I assume a path integral of appropriate form and show how the mean-field equation follows from it. Then I show how such a path integral follows from the Anderson lattice model when one imposes the above restrictions. I specialize to spin $\frac{1}{2}$ for clarity; the generalization to higher spin is straightforward but technically very messy. Moreover, the high-spin case with realistic treatment of the hybridization will have a very complicated RKKY interaction.[71]

The path integral which gives rise to (4.1) and (4.2) is expressed in terms of the Lagrangian

$$\mathcal{L}(\tau)=\mathcal{L}_f(\tau)+\mathcal{L}_b(\tau)+\mathcal{L}^0_{fb}(t)+\mathcal{L}_{ff}(\tau)\ , \tag{A1}$$

with

$$\mathcal{L}_f(\tau)=\sum_{\sigma\mathbf{R}} f^*_{\mathbf{R}\sigma}(\tau)\left[\frac{\partial}{\partial\tau}+\epsilon_f-\mu-\lambda_{\mathbf{R}}\right]f_{\mathbf{R}\sigma}(\tau)\ , \tag{A2a}$$

$$\mathcal{L}_b(\tau)=\sum_{\mathbf{R}} b^*_{\mathbf{R}}(\tau)\left[\frac{\partial}{\partial\tau}-\lambda_{\mathbf{R}}\right]b_{\mathbf{R}}(\tau)\ , \tag{A2b}$$

$$\mathcal{L}^0_{fb}(\tau)=\sum_{\mathbf{R}\sigma}\int_0^\beta d\tau' f^*_{\mathbf{R}\sigma}(\tau)b_{\mathbf{R}}(\tau)v_\sigma(0,\tau-\tau')b^*_{\mathbf{r}}(\tau')f_{\mathbf{R}\sigma}(\tau')\ , \tag{A2c}$$

$$\mathcal{L}_{ff}(\tau)=-\sum_{\mathbf{R}\neq\mathbf{R}'}\sum_{\mu\nu\rho\lambda} I(\mathbf{R}-\mathbf{R}')\mathbf{S}_{\mu\nu}\cdot\mathbf{S}_{\rho\lambda}f^{*}_{\mathbf{R}\mu}(\tau) \times f_{\mathbf{R}\nu}(\tau)f^{*}_{\mathbf{R}'\rho}(\tau)f_{\mathbf{r}'\lambda}(\tau)\ . \quad \text{(A2d)}$$

In the above, $\tau$ is a "thermal time" running from 0 to $\beta=1/k_BT$, and the $\{f_{\mathbf{R}\sigma},f^{*}_{\mathbf{R}\sigma}\}$ are anticommuting (Grassmann) variables antiperiodic on $[0,\beta]$ which correspond to the pseudofermion variables, the $\{b_{\mathbf{R}},b^{*}_{\mathbf{R}}\}$ are commuting variables periodic on $[0,\beta]$ which represent the pseudoboson fields, $\mu$ is the fermion chemical potential, $\mathbf{S}$ is a spin-$\frac{1}{2}$ matrix, $\lambda_{\mathbf{R}}$ is the pseudoparticle chemical potential at site $\mathbf{R}$, and the interaction function $v(\mathbf{R},\tau)$ is related to the conduction-electron propagator via [$\omega=(2n+1)\pi/\beta$, $n$ an integer]

$$v(\mathbf{R},\tau)=\frac{V^2}{\beta N_s}\sum_{\mathbf{k}n} e^{i(\mathbf{k}\cdot\mathbf{R}-\omega\tau)}\frac{1}{i\omega-\epsilon_k+\mu}\ . \quad \text{(A3)}$$

The path-integral representation of the partition function $Z(T)$ is then

$$Z(T)=Z_{\mathrm{CB}}(T)\prod_{\mathbf{R}}\frac{\partial}{\partial\zeta_{\mathbf{R}}}\int\exp\left[-\int_0^{\beta}d\tau\mathcal{L}(\tau)\right]\Bigg|_{\zeta_{\mathbf{R}}=0}, \quad \text{(A4)}$$

where $Z_{\mathrm{CB}}(T)$ is the normal conduction-band partition function, $\zeta_{\mathbf{R}}=e^{\beta\lambda_{\mathbf{R}}}$ is the pseudoparticle fugacity at site $\mathbf{R}$, and the symbol $\int$ is shorthand for the standard path-integral notation, i.e.,

$$\int=\prod_{\mathbf{R}}\int\left[\prod_{\sigma}Df^{*}_{\mathbf{R}\sigma}Df_{\mathbf{R}\sigma}\right]Db^{*}_{\mathbf{R}}Db_{\mathbf{R}}\ . \quad \text{(A5)}$$

The above expression for the path integral corresponds to that for a Wick rotated Lagrangian at finite temperature. For more details, see Ramond,[72] Sherrington,[73] and Read and Newns.[74]

Note that in contrast to Read and Newns, who augmented the constraint by integrating over the pseudoparticle chemical potential (which amounts to an *inverse discrete Laplace transform* of the pseudopotential grand canonical partition function to the canonical space with fixed $Q=1$), I have done the projection by the same method utilized in the self-consistent approach. The separate methods give the same results, of course, if the $\lambda$ integrals are done exactly.

Note that apart from the chemical potential effects tacit in (A4) and the interaction term $\mathcal{L}_{ff}(\tau)$, (A4) is no different than a product of one-site partition functions. In the extreme Kondo limit, the $f$ occupancy is basically pinned to unity, independent of $\mu$ according to the friedel sum rule,[54] so the one-site physics will not be substantially modified.

The molecular field equation is derived as follows. (i) Rewrite the interaction term as

$$\mathcal{L}_{ff}(\tau)=\frac{-1}{2}\sum_{\mathbf{R}\neq\mathbf{R}'}I(\mathbf{R}-\mathbf{R}')\{[\mathbf{S}_{\mathbf{R}}(\tau)+\mathbf{S}_{\mathbf{R}'}(\tau)]^2 -\mathbf{S}^2_{\mathbf{R}}(\tau)-\mathbf{S}^2_{\mathbf{R}'}(\tau)\}\ , \quad \text{(A6)}$$

where $\mathbf{S}_{\mathbf{R}}(\tau)=\mathbf{S}_{\mu\nu}f^{*}_{\mathbf{R}\mu}(\tau)f_{\mathbf{R}\nu}(\tau)$. Note that the self-interaction terms so introduced may be subsequently dropped since they vanish in the physical subspace with unit pseudocharge at each site. Note also that based on experience with Hamiltonians, one might expect a one-body shift to arise out of (A6), but since the Grassmann fields square to zero, there is no idempotence as is true of fermion *operators*. (ii) For each bond introduce a magnetization field $\mathbf{M}(\mathbf{R}-\mathbf{R}',\tau)$ via the Hubbard-Stratanovich identity

$$\exp\{\tfrac{1}{2}I(\mathbf{R}-\mathbf{R}')[\mathbf{S}_{\mathbf{R}}(\tau)+\mathbf{S}_{\mathbf{R}'}(\tau)]^2\} =\int D\mathbf{M}(\mathbf{R}-\mathbf{R}')\exp(-2I(\mathbf{R}-\mathbf{R}')\{\mathbf{M}^2(\mathbf{R}-\mathbf{R}',\tau)+\mathbf{M}(\mathbf{R}-\mathbf{R}',\tau)\cdot[\mathbf{S}_{\mathbf{R}}(\tau)+\mathbf{S}_{\mathbf{R}'}(\tau)]\})\ . \quad \text{(A7)}$$

(iii) Assume a preferred direction $\hat{z}$ and neglect transverse fluctuations. Make the static, uniform approximation for a spontaneous magnetization $\mathbf{M}$. Then one simply includes a molecular field shift to the pseudofermion levels

$$\mathcal{L}_{mf}(\tau)=-\sum_{\mathbf{R}}\lambda\mathbf{M}\sigma f^{*}_{\mathbf{R}\sigma}(\tau)f_{\mathbf{R}\sigma}(\tau) \quad \text{(A8)}$$

with

$$\lambda=2\sum_{\mathbf{R}\neq 0}I(\mathbf{R})\ . \quad \text{(A9)}$$

(iv) Evaluate the resulting free energy and extremize with respect to $\mathbf{M}$. The resulting free energy is precisely that of Eq. (4.1) for spin $\frac{1}{2}$, and clearly the same extremization condition (4.2) applies as well.

Having demonstrated how (4.1) follows from an appropriate path integral, I now show how (A4) can follow from the degenerate Anderson lattice model. The strategy is to write the lattice partition function in terms of the pseudoparticle variables, and then to integrate out the boson variables. This will give an effective action for the fermion variables which contains both on-site and intersite corrections. The intersite corrections may be explicitly separated and perturbatively expanded giving a result reminiscent of the linked cluster theorem. Truncating at the two-site level with neglect of the dynamics of the interaction function and of self-energy corrections to the pseudoboson propagators contained therein results in a partition function of the form (A4) provided one reintroduces boson variables for the on-site terms. What these approximations omit are (i) coherence effects which arise in two-particle fermion propagators from all possible conduction-electron self-energy insertions, (ii) the possibility of multisite Kondo effects by ignoring the dynamics of the two-site interactions, and (iii) the inclusion of "anomalous" RKKY terms due to the Kondo effect when boson self-energy corrections are ignored. Of these omissions, (i) and (ii) are serious, at least at low enough temperature

scales, while (iii) is apparently not so serious, as indicated in Appendix B. I now proceed with the formal details.

Upon integration of conduction variables, the Anderson-lattice partition function $Z_{\rm AL}$ has the general structure of (A4) with the Lagrangian $\mathcal{L}$ replaced by

$$\mathcal{L}_{\rm AL}(\tau)=\mathcal{L}(\tau)-\mathcal{L}_{ff}(\tau)+\mathcal{L}^{I}_{fb}(\tau)\ , \tag{A10}$$

with

$$\mathcal{L}^{I}_{fb}(\tau)=\sum_{\mathbf{R}\neq\mathbf{R}',\sigma}\int_0^\beta d\tau' f^{*}_{\mathbf{R}\sigma}(\tau)b_{\mathbf{R}}(\tau)v_\sigma(\mathbf{R}-\mathbf{R}',\tau-\tau') \times b^{*}_{\mathbf{R}'}(\tau')f_{\mathbf{R}'\sigma}(\tau')\ . \tag{A11}$$

In order to proceed further it is convenient to switch from the time domain to the frequency domain. The appropriate variable transformations are

$$f_{\mathbf{R}\sigma}(\tau)=\sum_n f_{\mathbf{R}\sigma}(\omega_n)e^{-i\omega_n\tau}\ , \tag{A12a}$$

$$v_\sigma(\mathbf{R},\tau)=\sum_n v_\sigma(\mathbf{R},\omega_n)e^{-\omega_n\tau}\ , \tag{A12b}$$

$$b_{\mathbf{R}}(\tau)=\sum_m b_{\mathbf{R}}(\nu_m)e^{-i\nu_m\tau}\ . \tag{A12c}$$

Here, of course, $\omega_n=(2n+1)\pi/\beta$; $\nu_m=2m\pi/\beta$.

With these replacements into (A11), I denote the resulting Lagrangians in the frequency domain with an overtilde, e.g., $\tilde{\mathcal{L}}_f$ is just the integral over $\mathcal{L}_f(\tau)$ along the imaginary time axis, viz.,

$$\tilde{\mathcal{L}}_f=\beta\sum_{n\sigma\mathbf{R}} f^{*}_{\mathbf{R}\sigma}(\omega_n)f_{\mathbf{R}\sigma}(\omega_n)(-i\omega_n+\epsilon_f-\lambda_{\mathbf{R}}-\mu)\ . \tag{A13}$$

Upon interating out the boson variables in (A11) then one obtains

$$Z_{\rm AL}(T)=Z_{\rm CB}(T)\times\prod_{\mathbf{R}}\frac{\partial}{\partial\zeta_{\mathbf{R}}}\int_f\exp\{-[\tilde{\mathcal{L}}_f-\mathrm{Tr}\ln\hat{D}_0+\mathrm{Tr}\ln(1-\hat{D}_0\hat{\pi}_I)]\}\,|_{\zeta_{\mathbf{R}}}\ , \tag{A14}$$

with $\int_f$ signifying the integration over the pseudofermion variables only, with the on-site boson propagator matrix

$$(\hat{D}_0)_{mm'\mathbf{R}\mathbf{R}'}=\delta_{\mathbf{R}\mathbf{R}'}\left[\delta_{mm'}(i\nu_m+\lambda_{\mathbf{R}})-\sum_{n\sigma}f^{*}_{\mathbf{R}\sigma}(\omega_n+\nu_m)v_\sigma(0,\omega_n)\times f_{\mathbf{R}\sigma}(\omega_n-\nu'_m)\right]^{-1}\ , \tag{A15}$$

the intersite boson self-energy matrix

$$(\hat{\tau}_l)_{mm'\mathbf{R}\mathbf{R}'}=(1-\delta_{\mathbf{R}\mathbf{R}'})\sum_{n\sigma}f^{*}_{\mathbf{R}\sigma}(\omega_n+\nu_m)v_\sigma(\mathbf{R}-\mathbf{R}',\omega_n)\times f_{\mathbf{R}'\sigma}(\omega_n-\nu'_m)\ , \tag{A16}$$

and the trace Tr denoting

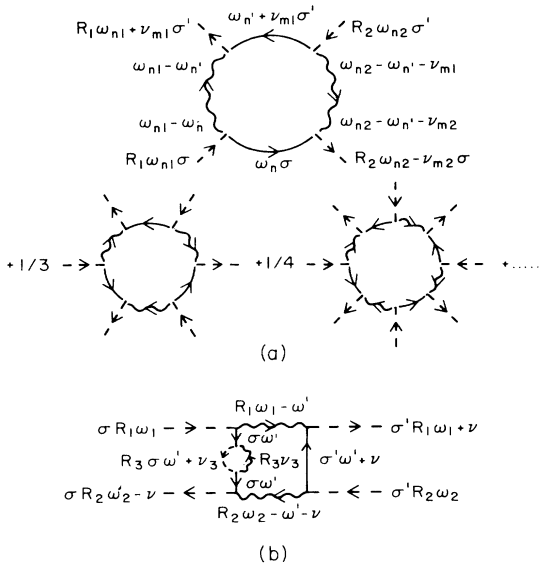


FIG. 11. Diagrammatics for the Anderson lattice partition function. (a) Perturbative expansion of the intersite logarithm [Eq. (A14)]. The dashed line represents a pseudofermion Grassmann variable; the wavy line the one-site pseudoboson propagator matrix [Eq. (A15)]; the solid line an intersite conduction propagator [Eq. (A12b)]. The $n$th order term in the expansion represents $n$-site pseudofermion exchange, and there is a corresponding weight factor of $1/n$ out front. Note that the pseudoboson propagator actually contains an infinite series of on-site retarded pseudofermion interactions in its self-energy. (b) Contribution to the two-particle pseudofermion propagator from three-site exchange. The intermediate fermion Lines are closed to make a self-energy insertion to the conduction-electron lines. The sum of all such possible insertions with proper accounting of site exclusion gives the coherent modification of the conduction propagators (Ref. 83) and hence of the RKKY interaction. At present, there is no reliable estimate of the effect of this coherent modification upon the RKKY interaction.

$$\mathrm{Tr}=\sum_{\mathbf{R}\mathbf{R}'mm'}\delta_{\mathbf{R}\mathbf{R}'}\delta_{mm'}\ . \tag{A17}$$

Note that $\tilde{\mathcal{L}}_f-\mathrm{Tr}\ln(\hat{D}_0)$ is precisely the exponent one would have for an incoherent produce of one-site partition functions with the $b$ fields traced over. Hence, to begin to put (A14) in the form (A4), I reintroduce $b$ variables at each site to the left of the intersite term.

Next, I expand the intersite term in (A14) in powers of the intersite self-energy. In view of the site restriction factor in (A16), only the even terms survive the expansion. The even terms are readily interpretable in terms of multisite pseudofermion interactions as indicated in Fig. 11(a). I truncate the expansion at the two-site level. Aside from removing the complication of exchange involving three and more sites, which to my knowledge have demonstrable importance so far only in solid $^3$He (Ref. 75) and have only recently been detected in a magnetic material (Ref. 76), the more serious omission is of the coherent modification of the RKKY interaction between two sites. This statement is clarified by examining Fig. 11(b), where

a two-particle pseudofermion propagator is shown with a single conduction-electron self-energy insertion obtained by closing one set of fermion legs on the three-site diagram of Fig. 11(a). At this point, I have no way to gauge the importance of such effects.

It remains to examine the structure of the two-site interaction function. The contribution to the Lagrangian of (A14) is $\tilde{\mathcal{L}}_{ff}$ equal to

$$-\frac{\beta}{2}\sum_{n,m}\sum_{\mathbf{R}_1\neq\mathbf{R}_2}\sum_{\sigma\sigma'} I(\nu_{m1},\nu_{m2},\omega_{n1},\omega_{n2}) f^{*}_{\mathbf{R}_1\sigma}(\omega_{n1}+\nu_{m1}) f^{*}_{\mathbf{R}_2\sigma'}(\omega_{n2}-\nu_{m2}) f_{\mathbf{R}_2\sigma}(\omega_2) f_{\mathbf{R}_1\sigma'}(\omega_1) , \tag{A18}$$

with $n,m$ in the first sum being shorthand for summing over all internal frequencies, and with

$$I(\nu_{m1},\nu_{m2},\omega_{n1},\omega_{n2}) = \frac{1}{\beta}\sum_{nn'}[\hat{D}_0(\omega_{n1}-\omega_n,\omega_{n1}-\omega_{n'},\mathbf{R}_1)\hat{D}_0(\omega_{n2}-\omega_{n'}-\nu_{m1},\omega_{n2}-\omega_n-\nu_{m2},\mathbf{R}_2) v_\sigma(\mathbf{R}_{12},\omega_n) v_{\sigma'}(\mathbf{R}_{21},\omega_{n'}+\nu_{m1})] , \tag{A19}$$

where $\mathbf{R}_{12}=-\mathbf{R}_{21}=\mathbf{R}_1-\mathbf{R}_2$. Note that (A18) may be broken up into intersite charge and spin interactions. I shall drop the charge interactions as those are not of interest here.

The reduction of (A18) and (A19) to the usual RKKY interaction follows in two steps. (a) Neglect the fermion contributions (self-energy) to $\hat{D}_0$, i.e., approximate

$$\hat{D}_0(m1,m2,\mathbf{R}) \approx \frac{\delta_{\nu_{m1}\nu_{m2}}}{i\nu_{m1}+\lambda_{\mathbf{R}}} . \tag{A20}$$

(b) Since in practice, the pseudofermion Green's function will be peaked about $\epsilon_f-\lambda_{\mathbf{R}}$, then the relevant frequencies $i\omega_{n1}$ and $i\omega_{n2}$ are $\epsilon_f-\lambda_{\mathbf{R}_1}$ and $\epsilon_f-\lambda_{\mathbf{R}_2}$, respectively. Thus, one can replace, e.g.,

$$\hat{D}_0(\omega_{n1}-\omega,\omega_{n1}-\omega',\mathbf{R}) \approx \frac{\delta_{\omega,\omega'}}{\epsilon_f} . \tag{A21}$$

Hence, a simplified form for $I$ is obtained which is

$$I(\nu_{m1},\nu_{m2},\omega_{n1},\omega_{n2}) \approx \delta_{\nu_{m1},\nu_{m2}}\frac{J_{cs}^2}{N_s^2}\sum_{\mathbf{k}\mathbf{k}'} e^{i(\mathbf{k}-\mathbf{k}')\cdot(\mathbf{R}_1-\mathbf{R}_2)}\frac{f(\epsilon_k)-f(\epsilon_{k'})}{i\nu_{m1}-\epsilon_k+\epsilon_{k'}} , \tag{A22}$$

where $J_{cs}=V^2/\epsilon_f$ is the Schrieffer-Wolff exchange integral, and $f(\epsilon)=1/(e^{\beta\epsilon}+1)$. Since only maximal frequency transfers of order $T_L$ are expected to be relevant, and since $I$ will vary for frequencies on the order of the conduction bandwidth, I will drop the remaining frequency dependence. Then Fourier transforming the remaining terms back to the time domain will result in an effective Lagrangian precisely of the form (A1).

What is omitted by this last set of approximations? First, the self-energy corrections will give rise to anomalous contributions to the RKKY interaction. I argue in Appendix B on a perturbative basis that these terms are less relevant than the usual RKKY term. Second, once the molecular field approximation is made, any chance of obtaining two-site Kondo effects is lost. The molecular field approximation corresponds to a particular way of decoupling the two-particle pseudofermion Green's functions which omits the higher-order dynamics that are supposed to give rise to two-site Kondo effects.

In summary, then, in this appendix I have shown that a Lagrangian of the appropriate form (A1) can be generated from the Anderson lattice provided one imposes restrictions (1)–(3) outlined at the beginning of this appendix. The restrictions taken together with the molecular field approximation eliminate the consideration of coherent modification of the RKKY interaction, three-site and higher exchange processes, boson self-energy effects on the two-site exchange process (a minor point), and the possibility of two-site Kondo effects.

## APPENDIX B

In this appendix I present a perturbative evaluation of the two-site RKKY interaction between Kondo impurities. The relevant diagram is shown in Fig. 12. I shall consider two impurities located at the origin and $\mathbf{R}$. I shall take the static limit and evaluate the energies of the pseudofermion legs at $\epsilon_f-\lambda_0$ and $\epsilon_f-\lambda_{\mathbf{R}}$. Denoting this limiting value of the interaction function by $I_0(\mathbf{R})$, I find

$$I_0(\mathbf{R}) = 2\frac{V^4}{N_s^2}\sum_{\mathbf{k}\mathbf{k}'} e^{i(\mathbf{k}-\mathbf{k}')\cdot\mathbf{R}}\frac{f(\epsilon_k)}{\epsilon_k-\epsilon_{k'}}[\mathrm{Re}D(\epsilon_f-\epsilon_k)]^2 , \tag{B1}$$

where the pseudoboson propagator $D(\nu)$ is defined in Eq. (2.11).

It is reasonable to approximate $\mathrm{Re}D(\epsilon_f-\epsilon_k)$ by a two-pole form, one contribution coming from the slow charge fluctuations peaked about $\epsilon_f$, and one from the rapid spin fluctuations peaked near $T_L$. Roughly, at $T=0$ K,

$$\mathrm{Re}D(\epsilon_f-\epsilon_k) \approx -\left[\frac{1}{|\epsilon_f|}+\frac{\alpha(\pi T_L/2\Gamma)}{\epsilon_k-\alpha T_L}\right] , \tag{B2}$$

where $\alpha$ is a factor of order unity. Substituting (B2) into (B1) and evaluating the resulting integrals gives

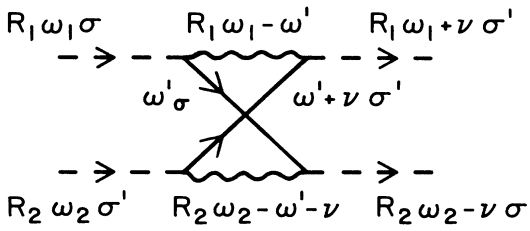


FIG. 12. Two pseudofermion propagator intersite self-energy diagram. The simplest intersite contribution to the two pseudofermion propagator self-energy is interpreted as the RKKY interaction between the pseudofermions. Note here that the wavy line represents the pseudoboson propagator given by Eq. (2.11).

$$I_0(\mathbf{R}) \approx \frac{\pi}{2} D \left[ [N(0)J_{cs}]^2 F_0(k_F R) + \frac{4\alpha T_L}{D} [N(0)J_{cs}] F_1(k_F R) + \frac{\alpha T_L}{2D} F_2(k_F R) \right] , \tag{B3}$$

where $J_{cs}$ is given below (A20) in Appendix A and the range functions are given by

$$F_0(k_F R) \approx \frac{\cos(2k_F R)}{(k_F R)^3} , \quad k_F^{-1} \ll R , \tag{B4a}$$

$$F_1(k_F R) \approx \frac{D}{4\alpha T_L} F_0(k_F R) , \quad \frac{v_F}{\alpha T_L} = \xi_K \ll R$$

$$\approx \frac{\left[ \frac{\pi}{2} - \mathrm{Si}(2R/\xi_K) \right] \cos(2k_F R) - \mathrm{Ci}(2R/\xi_K) \sin(2k_F R)}{(k_F R)^2} , \quad k_F^{-1} \ll R \ll \xi_K \tag{B4b}$$

where $\mathrm{Si}(x)$ and $\mathrm{Ci}(x)$ are the sine and cosine integral functions,[77] $v_F$ is the Fermi velocity of the normal conduction states, $\xi_K$ is the so-called "Kondo coherence length," and finally

$$F_2(k_F R) \approx \frac{D}{2\alpha T_L} F_0(k_F R) , \quad \xi_K \ll R$$

$$\approx \frac{\sin(2k_F R)}{(k_F R)^2} , \quad k_F^{-1} \ll R \ll \xi_K . \tag{B4c}$$

Noting that $N(0)J_{cs}$ is perturbatively small, and therefore that $T_L/D \sim \exp[-1/|N(0)J_{cs}|]$ is even smaller, I can collect terms and see that

$$I_0(\mathbf{R}) \approx \frac{\pi}{2} D \{ [N(0)J_{cs}] + \tfrac{1}{2} \}^2 F_0(k_F R) , \quad \xi_K \ll R$$

$$\approx \frac{\pi}{2} D \left[ [N(0)J_{cs}]^2 F_0(k_F R) + \frac{\alpha T_L}{2D} [N(0)J_{cs}] F_1(k_F R) \right] , \quad k_F^{-1} \ll R \ll \xi_K . \tag{B5}$$

Clearly, the anomalous terms arising from (B4b) and (B4c) dominate the interaction only for $R \gg \xi_K$. Since $T_L \to 0$ is usually the relevant limit for considerations of magnetic order, and since (a) $\xi_K \to \infty$ in that limit and (b) any mean-free-path effects at finite temperatures will tend to cut off the range functions at the mean free path $l$ which will likely be much smaller than $\xi_K$ at any reasonable temperature, I conclude that the normal RKKY interactions (proportional to $J_{cs}^2$ above) are the most crucial in determining magnetic order.

I note that while other workers have obtained the same results for the anomalous terms,[49,78–80] I am unaware of any who have clearly pointed out the dominance of the regular RKKY terms in this fashion. Lee[79] and Rasul and Hewson[80] were the first to use the breakup of the pseudoboson propagator within large-$N_{\mathrm{grd}}$ theory according to the form (B2). Ishii has reached similar conclusions using perturbation theory in $U/\pi\Gamma$, where $U$ is the Coulomb repulsion between up- and down-spin electrons.[81]

*Present and permanent address: Department of Physics, Ohio State University, 174 W. 18th Avenue, Columbus, OH 43210.

[1]P. W. Anderson, Phys. Rev. **124**, 41 (1961).
[2]H. Keiter and J. C. Kimball, Int. J. Magn. **1**, 233 (1971).
[3]S. Inagaki, J. Magn. Magn. Mater. **15-18**, 951 (1980).
[4]H. Keiter and G. Czycholl, J. Magn. Magn. Mater. **31**, 477 (1983).
[5]Y. Kuramoto, Z. Phys. B **53**, 37 (1983).
[6]F. C. Zhang and T. K. Lee, Phys. Rev. B **33**, 33 (1983).
[7]N. Grewe, Z. Phys. B **53**, 271 (1983).
[8]P. Coleman, Phys. Rev. B **29**, 3035 (1984).
[9]N. E. Bickers, D. L. Cox, and J. W. Wilkins, Phys. Rev. Lett. **54**, 230 (1985).
[10]P. Schlottmann, J. Magn. Magn. Mater. **52**, 214 (1985).
[11]D. L. Cox, N. E. Bickers, and J. W. Wilkins, J. Appl. Phys. **57**, 3166 (1985).
[12]D. L. Cox, N. E. Bickers, and J. W. Wilkins, J. Magn. Magn. Mater. **54-57**, 333 (1986).
[13]H. Kojima, Y. Kuramoto, and M. Tachiki, Z. Phys. B **54**, 293 (1984).
[14]K. G. Wilson, Rev. Mod. Phys. **47**, 773 (1975).
[15]H. R. Krishna-Murthy, J. W. Wilkins, and K. G. Wilson, Phys. Rev. B **21**, 1003 (1980); **21**, 1044 (1980).
[16]N. Andrei, K. Furuya, and J. H. Lowenstein, Rev. Mod. Phys. **55**, 331 (1983).
[17]P. B. Wiegmann, Pis'ma Zh. Eksp. Teor. Fiz. **31**, 392 (1980) [JETP Lett. **31**, 364 (1980)].
[18]V. T. Rajan, Phys. Rev. Lett. **51**, 308 (1983).
[19]A. C. Hewson and J. W. Rasul, J. Phys. C **16**, 6799 (1983).
[20]N. Kawakami and A. Okiji, J. Appl. Phys. **55**, 1931 (1984).
[21]P. Schlottmann, Z. Phys. B **56**, 127 (1984).
[22]J. W. Rasul and A. C. Hewson, J. Phys. **17**, 3337 (1984).

[23]F. C. Zhang and T. K. Lee, Phys. Rev. B **30**, 1556 (1984).
[24]Y. Onuki, Y. Furukawa, and T. Komatsubara, J. Phys. Soc. Jpn. **53**, 2734 (1984).
[25]P. A. Lee, T. M. Rice, J. W. Serene, L. J. Sham, and J. W. Wilkins, Comments Condens. Matter Phys. **12**, 99 (1986). The data referenced was taken by Lin *et al.* See Ref. 25(b) of this review.
[26]P. Coleman, Phys. Rev. B **28**, 5255 (1983).
[27]K. Yamada, K. Yosida, and K. Hanzawa, Prog. Theor. Phys. **71**, 450 (1984).
[28]N. Read, D. M. Newns, and S. Doniach, Phys. Rev. B **30**, 3841 (1984).
[29]K. Ueda and T. M. Rice, Phys. Rev. Lett. **55**, 995 (1985).
[30]B. Brandow, Phys. Rev. B **33**, 215 (1986).
[31]C. D. Bredl, S. Horn, F. Steglich, B. Luthi, and R. M. Martin, Phys. Rev. Lett. **52**, 1982 (1984).
[32]G. R. Stewart, Rev. Mod. Phys. **56**, 755 (1984).
[33]J. M. Lawrence, P. S. Riseborough, and R. D. Parks, Rep. Prog. Phys. **44**, 1 (1981).
[34]S. K. Malik, G. K. Shenoy, S. M. Heald, and S. M. Tranquada, Phys. Rev. Lett. **55**, 316 (1985).
[35]S. A. Shaheen, M. Abd-Elmeguid, H. Micklitz, J. S. Schilling, P. Klavins, and R. N. Shelton, Phys. Rev. Lett. **55**, 312 (1985).
[36]C. D. Bredl, F. Steglich, and K. D. Schotte, Z. Phys. B **29**, 327 (1977).
[37]A. Benoit, J. Flouquet, M. Ribault, F. Flouquet, G. Chouteau, and R. Tournier, J. Phys. (Paris) Lett. **39**, L94 (1978).
[38]J. M. Effantin, J. Rossat-Mignod, P. Burlet, H. Bartholin, S. Kunii, and T. Kasuya, J. Magn. Magn. Mater. **47-48**, 145 (1985).
[39]C. L. Lin, T. Mihalism, and J. Crow, Phys. Rev. Lett. **54**, 2541 (1985).
[40]J. Lawrence, J. Appl. Phys. **53**, 2117 (1982).
[41]M. B. Maple, S. E. Lambert, M. S. Torikachvili, K. N. Yang, J. W. Allen, B. B. Pate, and I. Lindau, J. Less-Common Met. **111**, 239 (1985).
[42]H. R. Ott, H. Rudigier, P. Delsing, and Z. Fisk, Phys. Rev. Lett. **52**, 1551 (1984).
[43]D. E. Cox, G. Shirane, S. Shapiro, G. Aeppli, Z. Fisk, J. L. Smith, J. Kjems, and H. R. Ott, Phys. Rev. B **33**, 3614 (1986).
[44]J. Lawrence and S. Shapiro, Phys. Rev. B **22**, 4379 (1980).
[45]I thank M. Norman for pointing this out to me.
[46]S. Doniach, in *Valence Instabilities and Related Narrow Band Phenomena,* edited by R. D. Parks (Plenum, New York, 1977), p. 169.
[47]R. Scalettar, D Scalapino, and R. Sugar, Phys. Rev. B **31**, 7316 (1985).
[48]C. Jayaprakash, H. R. Krishna-murthy, and J. W. Wilkins, Phys. Rev. Lett. **47**, 737 (1981).
[49]C. Jayaprakash, H. R. Krishna-murthy, and J. W. Wilkins, J. Appl. Phys. **53**, 2142 (1982).
[50]R. M. Martin and J. W. Allen, J. Appl. Phys. **50**, 7561 (1979).
[51]J. H. Lowenstein, Phys. Rev. B **29**, 4120 (1984).
[52]S. E. Barnes, J. Phys. F **6**, 1375 (1976).
[53]N. Andrei and J. Lowenstein, Phys. Rev. Lett. **46**, 356 (1981).
[54]D. C. Langreth, Phys. Rev. **150**, 516 (1966).
[55]For a detailed discussion of the high-field perturbation theory, see Ref. 16, Appendix A.
[56]D. M. Newns, N. Read, and A. C. Hewson, in *Moment Formation in Solids,* edited by W. J. M. Buyers (Plenum, New York, 1984), p. 257.
[57]W. C. M. Mattens, in Ph.D. thesis, University of Amsterdam, (1980).
[58]A. C. Hewson, J. W. Rasul, and D. M. Newns, Solid State Commun. **47**, 59 (1983).
[59]A. Okiji and N. Kawakami, J. Magn. Magn. Mater. **54-57**, 327 (1986).
[60]J. W. Allen and R. M. Martin, Phys. Rev. Lett. **49**, 1106 (1982).
[61]P. Schlottmann, J. Appl. Phys. **57**, 3155 (1985).
[62]N. E. Bickers, D. L. Cox, and J. W. Wilkins, J. Magn. Magn. Mater. **47-48**, 335 (1985).
[63]J. F. Herbst, J. Magn. Magn. Mater. **47-48**, 238 (1985).
[64]M. Schöpner, J. Moser, A. Kratzer, U. Potzel, J. M. Mignot, and G. M. Kalvius, Z. Phys. B **63**, 25 (1986).
[65]H. E. Stanley, in *Introduction to Phase Transitions and Critical Phenomena* (Oxford University Press, New York, 1971), p. 172.
[66]I thank M. Thorpe and T. Kaplan for bringing this point to my attention.
[67]K. Yang (private communication).
[68]G. Czycholl, Phys. Rev. B **31**, 2867 (1985).
[69]H. Suhl, Phys. Rev. Lett. **55**, 2999 (1985).
[70]B. Jones, C. Varma, and E. Abrahams (unpublished).
[71]R. Siemann and B. R. Cooper, Phys. Rev. Lett. **44**, 1015 (1980).
[72]P. Ramond, in *Field Theory, A Modern Primer* (Benjamin/Cummings, Reading, Mass., 1982), Chaps. II and V.
[73]D. Sherrington, J. Phys. C **4**, 401 (1971).
[74]N. Read and D. M. Newns, J. Phys. C **16**, 3273 (1983).
[75]M. C. Cross and D. S. Fisher, Rev. Mod. Phys. **57**, 881 (1985).
[76]U. Falk, A. Furrer, H. U. Güdel, and J. K. Kjems, Phys. Rev. Lett. **56**, 1956 (1986).
[77]M. Abramowitz and I. A. Stegun, in *Handbook of Mathematical Functions* (Dover, New York, 1972), p. 231.
[78]A. M. Tsvelic, Zh. Eksp. Teor. Fiz. **76**, 2260 (1979) [Sov. Phys.—JETP **49**, 1142 (1979)].
[79]T. K. Lee, J. Phys. C **18**, 31 (1985).
[80]J. W. Rasul and A. C. Hewson, Solid State Commun. **52**, 217 (1984).
[81]H. Ishii, J. Low. Temp. Phys. **32**, 457 (1978).
[82]V. T. Rajan, J. H. Lowenstein, and N. Andrei, Phys. Rev. Lett. **49**, 497 (1982).
[83]N. Grewe, Solid State Commun. **50**, 19 (1984).